Radboud Universiteit Nijmegen

Charge carrier scattering and electronic transport in graphene
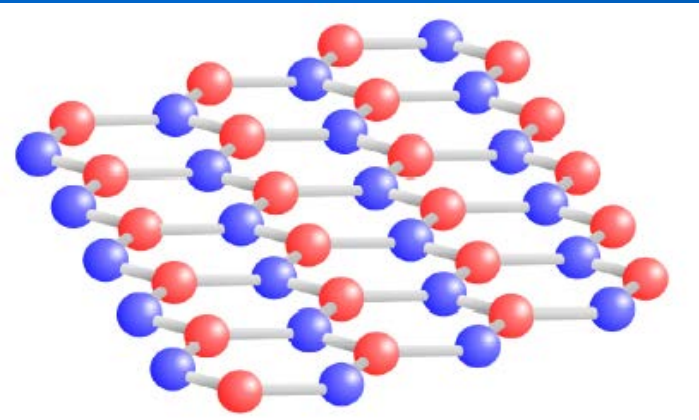
Mikhail Katsnelson

iMM

Institute for Molecules and Materials

Outline

1. *Minimal conductivity*
2. *Scattering by point defects: Boltzmann equation*
3. *Scattering by point defects: bilayer*
4. *Charge impurities and cluster formation*
5. *Resonant scatterers*
6. *Scattering by flexural phonons (ripples): main mechanism for suspended samples?*
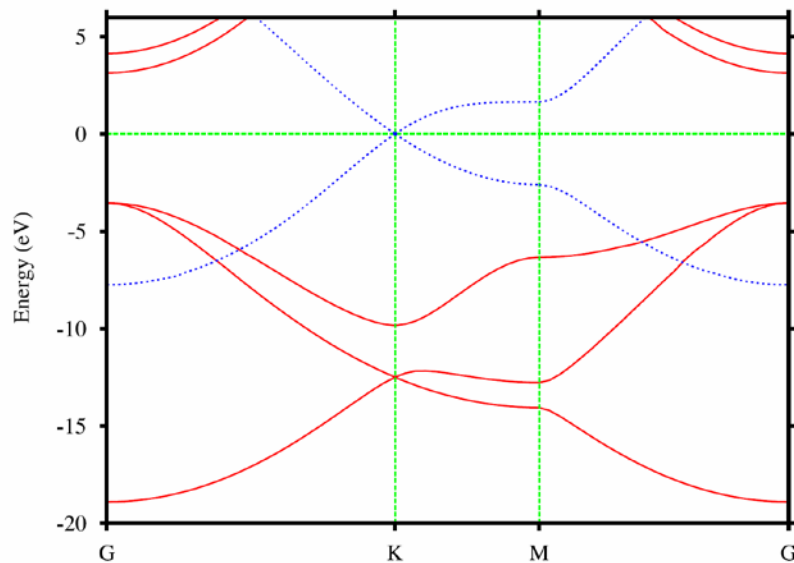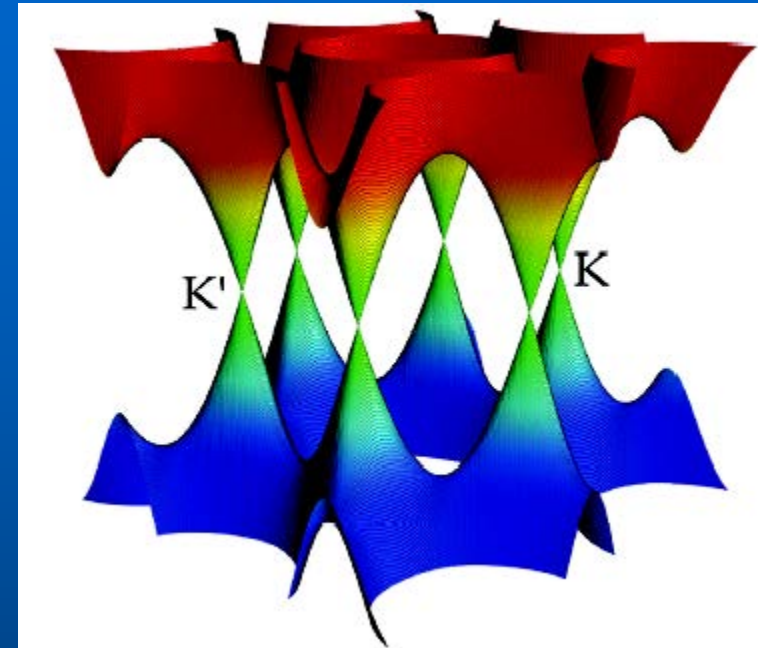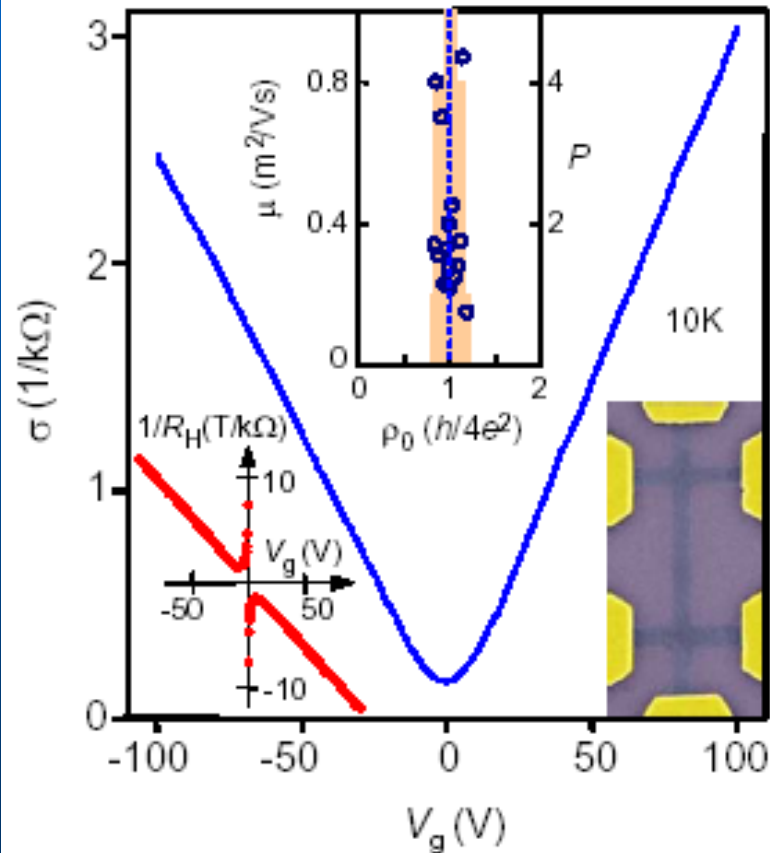
Massless Dirac fermions

pseudospin

sp^2 hybridization, π bands crossing the neutrality point

Neglecting intervalley scattering: massless Dirac fermions

Symmetry protected (*T* and *I*)

FIG. 2: (color online) Band structure of a single graphene layer. Solid red lines are σ bands and dotted blue lines are π bands.
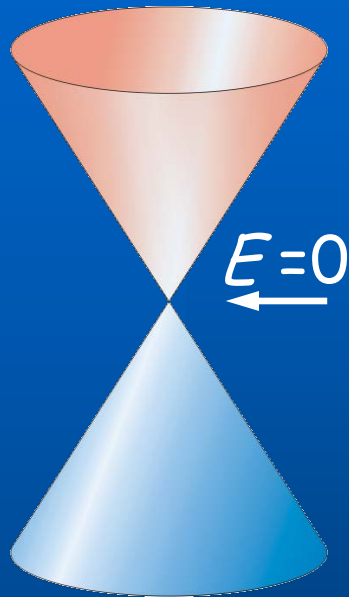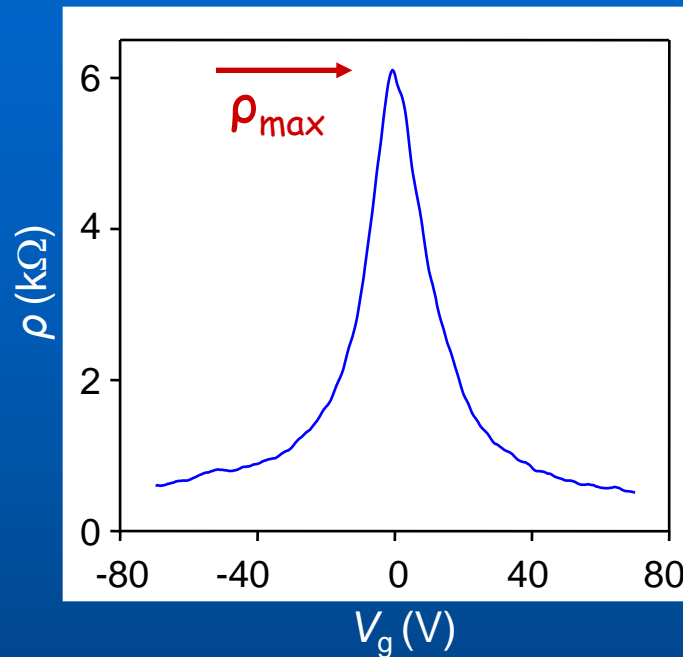
V-shape: to be explained

Minimal conductivity of the order of e^2/h per channel

Conductivity is approx. proportional to charge-carrier concentration n (concentration-independent mobility).
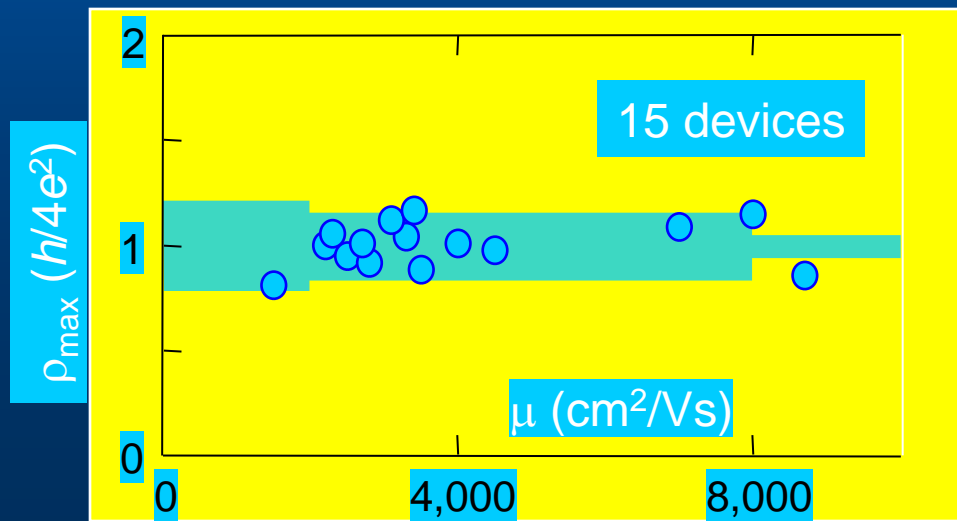
Novoselov et al, Nature 2005

Quantum-Limited Resistivity

no temperature
dependence
in the peak
between 3 and 80K

zero-gap
semiconductor

Novoselov et al,
Nature 2005

Transport via evanescent waves

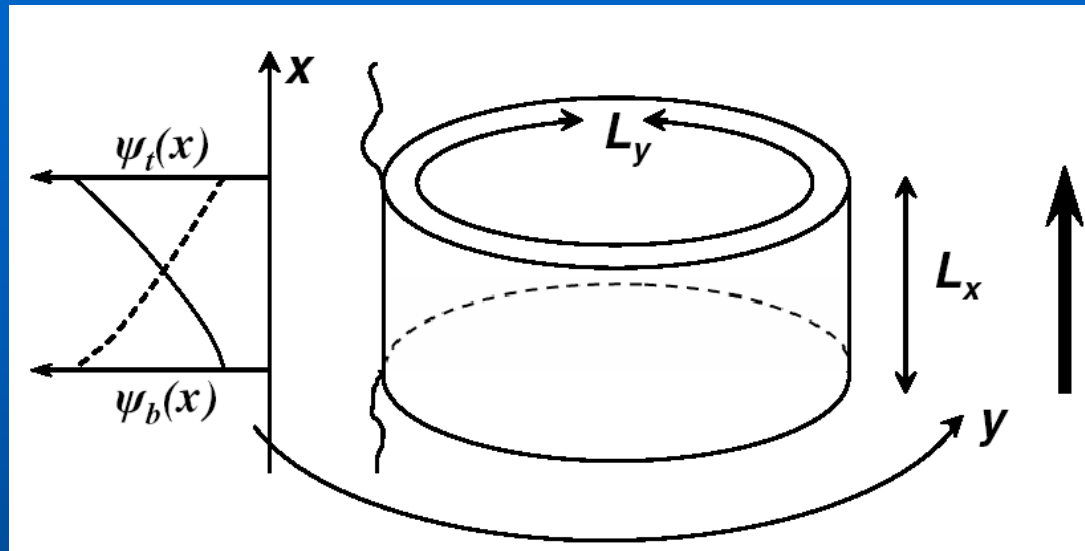Conductance $= e^2/h \; Tr \; T$ per valley per spin

T is the transmission probability matrix

The wave functions of massless
Dirac fermions at zero energy:

$$\left(\frac{\partial}{\partial x} \pm i \frac{\partial}{\partial y} \right) \psi_\pm(x, y) = 0 \qquad \psi_\pm(x, y) = f(x \pm iy) \qquad \forall f$$

Boundary conditions determine the functions f

Transport via evanescent waves II

$$\psi_\pm(x, y) = \exp\left[\frac{2\pi n}{L_y}(x \pm iy)\right] \qquad n = 0, \pm 1, \pm 2, \ldots$$

$f(y+L_y) = f(y)$ Edge states near the top and bottom of the sample

New type of electron transport: via evanescent waves – different from both ballistic and diffusive

Transport via evanescent waves III

Leads from doped graphene

$$T_n = |t(k_y)|^2 = \frac{\cos^2 \phi}{\cosh^2(k_y L_x) - \sin^2 \phi}$$

$$\sin \phi = k_y / k_F$$

$$Tr T = \sum_{n=-\infty}^{\infty} \frac{1}{\cosh^2(k_y L_x)} \simeq \frac{L_y}{\pi L_x}$$

Conductivity per channel: $e^2/(\pi h)$

The problem of "missing pi(e)" – may be, no problem

Transport via evanescent waves IV

Recent experiment

In very clean samples min conductivity is close to theor. prediction

How Close Can One Approach the Dirac Point in Graphene Experimentally?   *Nano Lett.* 2012, 12, 4629–4634

Alexander S. Mayorov,[*,†] Daniel C. Elias,[†] Ivan S. Mukhin,[‡] Sergey V. Morozov,[§] Leonid A. Ponomarenko,[†] Kostya S. Novoselov,[†] A. K. Geim,[†,‡] and Roman V. Gorbachev[†,‡]
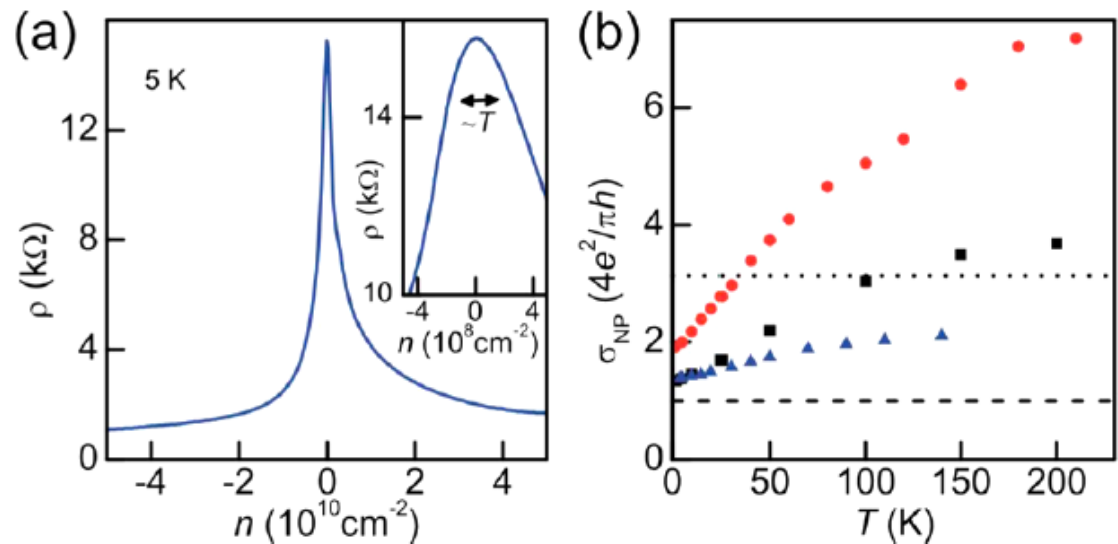
**Figure 3.** Height and broadening of the resistivity peak. (a) $\rho(n)$ for one of our devices. Inset: thermal smearing of the tip. (b) T dependence of σ at the NP for three devices. The dashed line indicates the ballistic limit; the dotted one is $4e^2/h$. For the sake of generality, no contact resistance is subtracted, which would result in slightly higher values of σ_{NP}.

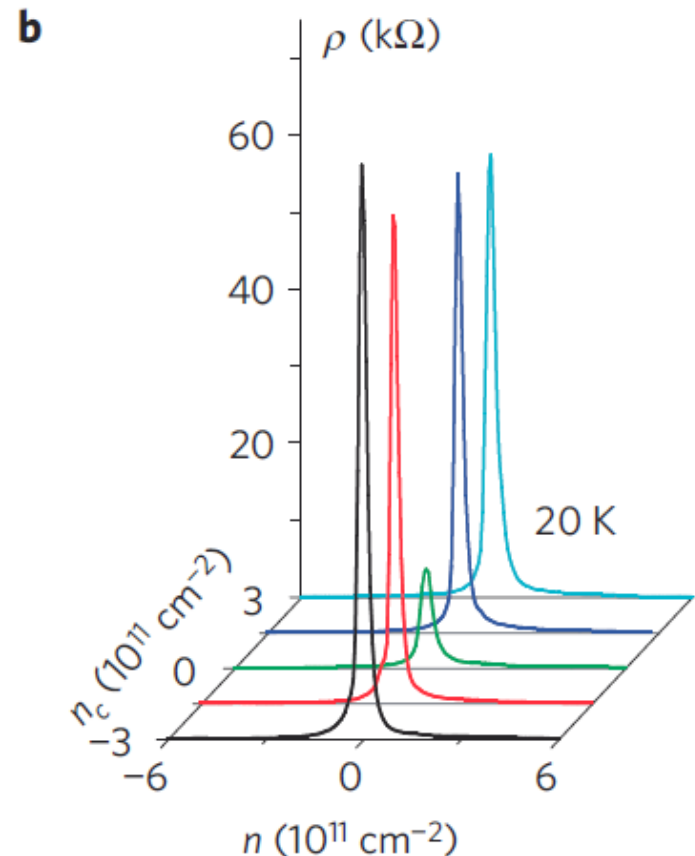# *Back to minimal conductivity*

Sometimes: conductivity much lower than e^2/h

[3] L. A. Ponomarenko, A. K. Geim, A. A. Zhukov, R. Jalil, S. V. Morozov, K. S. Novoselov, V. V. Cheianov, V. I. Fal'ko, K. Watanabe, T. Taniguchi, and R. V. Gorbachev, Nature Phys. **7**, 958 (2011).
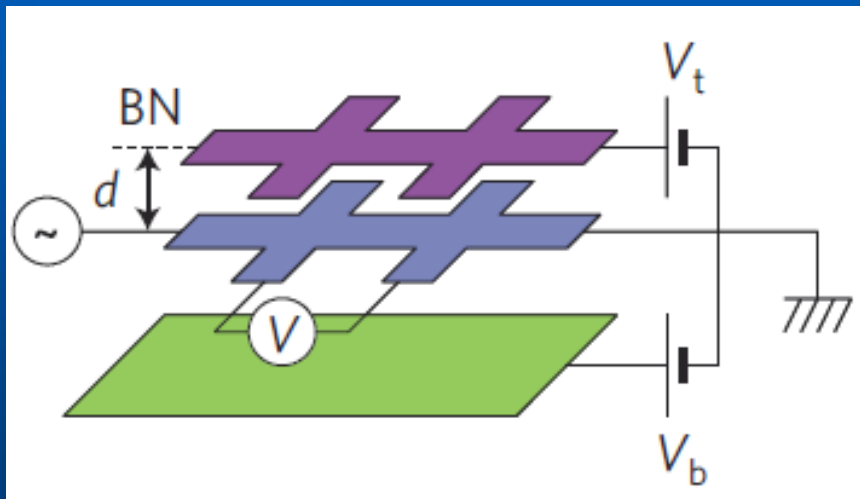
Graphene encapsulated in hBN.
Strong sensitivity to screening by
another graphene layer, temperature
and magnetic field

Another recent experiment

Insulating Behavior at the Neutrality Point in Single-Layer Graphene
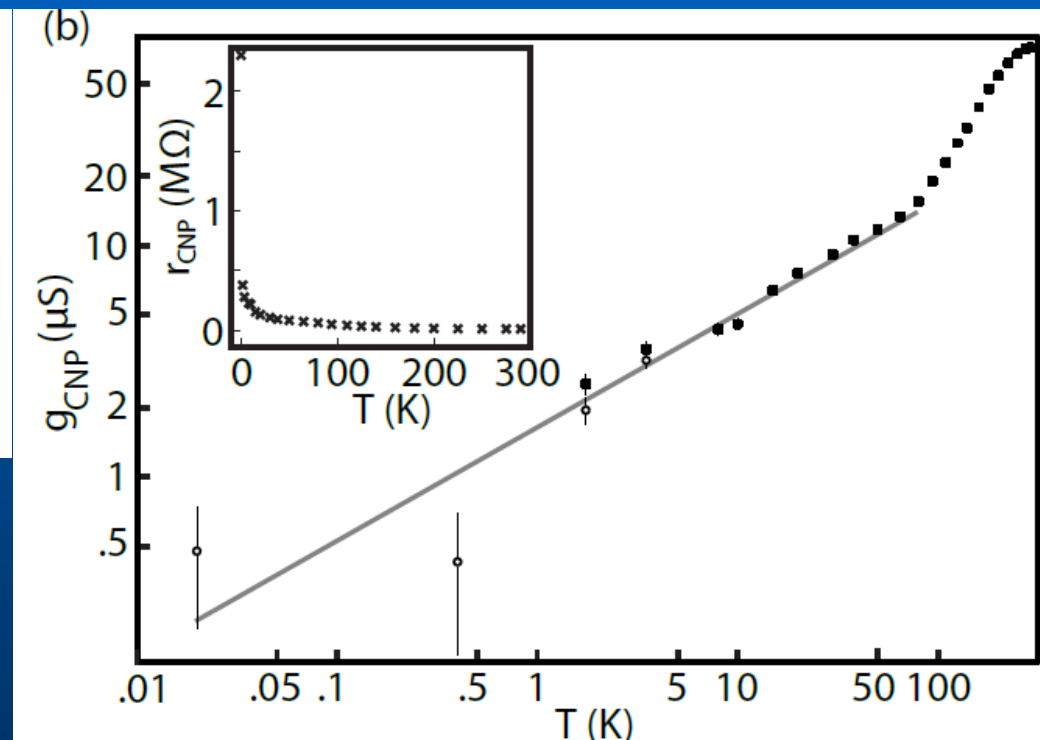
F. Amet,[1] J. R. Williams,[2] K. Watanabe,[3] T. Taniguchi,[3] and D. Goldhaber-Gordon[2]
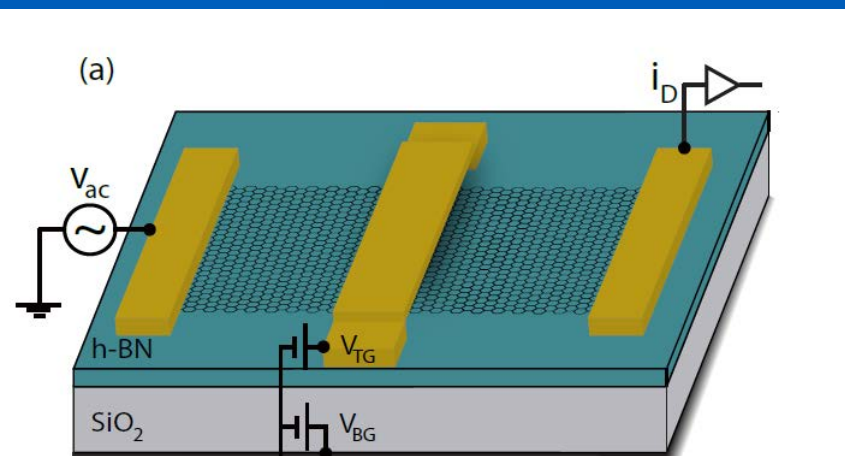
Also, graphene on hBN

Power-law behavior with temperature

$$g_{CNP} \propto T^{\alpha} \text{ with } \alpha \approx 0.48 \pm 0.05$$
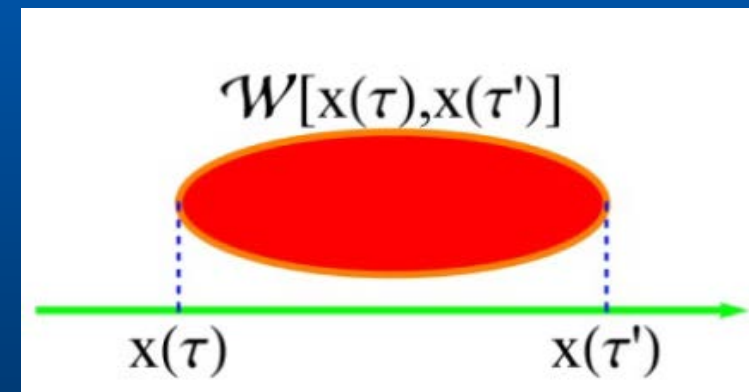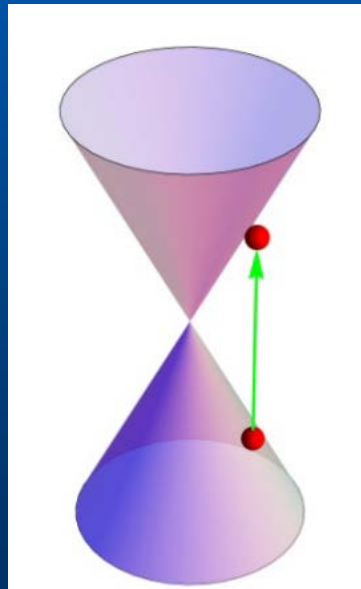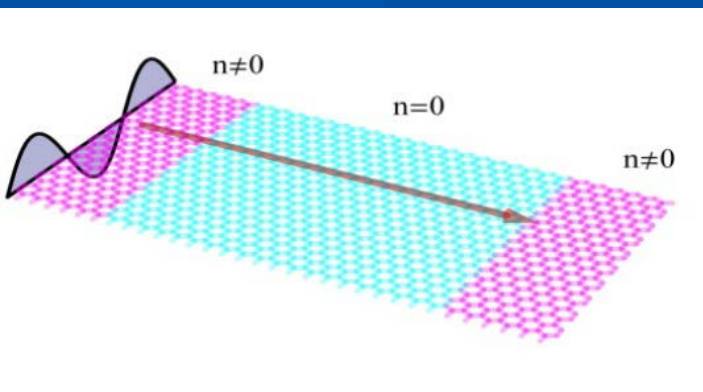
Many-body renormalization

F. Guinea & MIK, PRL 112, 116604 (2014)

Caldeira & Leggett, 1981, 1983: tunneling with dissipation

Overlap of the wave functions are suppresed by overlap
of the wave functions of environment (then, averaging over
the environment)

Transport via evanescent
waves is tunneling

Nonlocal self-interaction

e-h pairs as thermal bath

Many-body renormalization II

Correction to the effective tunneling action

$$\delta S = \frac{1}{2} \int_{-\infty}^{+\infty} d\tau \int_0^{\beta} d\tau' \int_{-\infty}^{+\infty} \frac{dq}{2\pi} \int_{-\infty}^{+\infty} d\omega \, e^{iq[x(\tau) - x(\tau') - \omega|\tau - \tau'|]} W(q, \omega)$$

Screened Coulomb interaction

$$W(q, \omega) = \frac{v_q}{\epsilon(q, \omega)}$$

Bare Coulomb interaction

$$v_q \simeq \begin{cases} -\frac{2e^2}{\epsilon_0} \log(qL_y) & qL_y \ll 1 \\ \frac{2\pi e^2}{\epsilon_0 qL_y} & 1 \ll qL_y \end{cases}$$

For undoped graphene

$$\epsilon(q, \omega) = 1 + v_q \chi_{1D}(q, \omega)$$

$$\chi_{1D}(q, \omega) \approx L_y \chi_{2D}(q, \omega) \approx L_y \frac{q^2}{4\sqrt{v_F^2 q^2 - \omega^2}}$$

Many-body renormalization III

Suppression of tunneling probability

$$T(k_y) \cong T_0(k_y) e^{-\delta S}$$

$$\delta S_G \approx \frac{L_x}{8\pi L_y} \frac{\alpha^2}{4\sqrt{2}+\alpha} \log\left(\frac{L_x}{a}\right)$$

for isolated graphene

In the presence of metallic layer:

$$g = k_F \ell$$

$$\chi_{1D}^M(q,\omega) \approx \begin{cases} \frac{v_{1D} D q^2}{i\omega + D q^2} & q \leq \ell^{-1} \\ \frac{v_{1D} v_F^M q}{i\omega + v_F^M q} & \ell^{-1} \leq q \leq k_F \end{cases}$$

$$\delta S_M = \delta S_d + \delta S_b \approx \frac{L_x^2}{4\pi g \ell L_y} + \frac{L_x}{8\pi L_y} \log(g)$$

Many-body renormalization IV

At finite temperatures the cut-off wave vector

$$q_c \approx \text{Max}(L_x^{-1}, T/\text{v}_F)$$
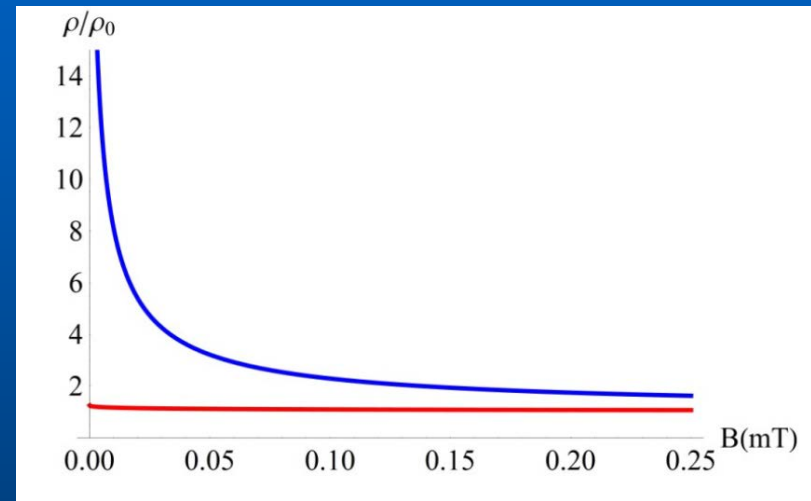
Magnetic field effects on diffusion!

T= 1K
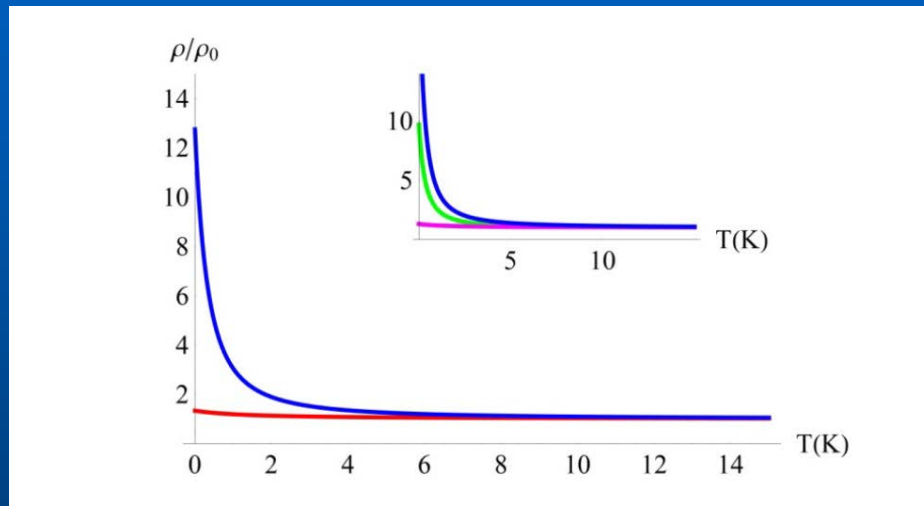
FIG. 2. Temperature dependence of the inverse conductance, normalized to the non interaction value, $\sigma_0 = e^2/(\pi\hbar)$, for $L_x = 4\mu$, $L_y = 1\mu$. Red: Contribution from the graphene excitations, δS_G, eq. 6. Blue: Contribution from a metallic layer, δS_M, eq. 8. The two terms which describe the contribution from the metal, δS_d and δS_b are shown in the inset. Green: diffusive part, δS_d in eq. 8. Magenta: ballistic part, δS_b in eq. 8. The carrier density in the metal is $n = 10^{11}\text{cm}^{-1}$, and the elastic mean free path is $\ell = 100\text{nm}$.

Scattering by point defects

$$\sigma = \frac{e^2}{h} 2\varepsilon_F \tau, \qquad \tau^{-1} = v_F n_{\mathrm{imp}} \sigma_{\mathrm{tr}}$$

$$\sigma_{\mathrm{tr}} = \int d\varphi (1 - \cos\varphi)|f(\varphi)|^2 = \frac{4}{k} \sum_{m=0}^{\infty} \sin^2\theta_m \qquad f(\varphi) = \frac{2i}{\sqrt{2\pi i k}} \sum_{m=0}^{\infty} (e^{2i\delta_m} - 1)\cos\left(m + \frac{1}{2}\right)\varphi$$

$$\theta_m = \delta_m - \delta_{m+1}$$

The back scattering $(\phi = \pi)$ is absent rigorously

(cf Klein tunneling)

s-scattering phase should be approx. constant at $k \to 0$; for a generic short-range potential it vanishes as kR (cf. optics). Long-range (or resonant) scattering is required

Justification of standard Boltzmann equation except very small doping:
$n >$ exp$(-\pi\sigma h/e^2)$, or $\varepsilon_F \tau >> 1/|\ln(k_F a)|$ (M.Auslender and MIK, PRB 2007)

Bilayer

Low-energy description:
Massive chiral fermions

$$H = \begin{pmatrix} 0 & -(p_x - ip_y)^2/2m \\ -(p_x + ip_y)^2/2m & 0 \end{pmatrix}$$

Constant DOS, no difference between charged and neutral impurities: short-range potential, anyway

$$V(q) = \frac{2\pi Ze^2}{\epsilon(q + \kappa)}$$

$$\kappa = 2\pi e^2 N(E_F) / \epsilon$$

Screening radius is about 4.5 Interatomic distances

Bilayer II

Radial wave equation:

$$\left(\frac{d}{dr} - \frac{l+1}{r}\right)\left(\frac{d}{dr} - \frac{l}{r}\right)g_l = \left(k^2 - \frac{2mV}{\hbar^2}\right)f_l,$$

$$\left(\frac{d}{dr} + \frac{l+1}{r}\right)\left(\frac{d}{dr} + \frac{l+2}{r}\right)f_l = \left(k^2 - \frac{2mV}{\hbar^2}\right)g_l,$$

$$l = 0, \pm 1, \ldots,$$

$g_l(r)e^{il\phi}$ and $f_l(r)e^{i(l+2)\phi}$ are spinor components

Bilayer III

Beyond the range of potential – not only scattered wave but also evanescent waves:

$$g_l(r) = A[J_l(kr) + t_l H_l^{(1)}(kr) + c_l K_l(kr)],$$

$$f_l(r) = A[J_{l+2}(kr) + t_l H_{l+2}^{(1)}(kr) + c_l K_{l+2}(kr)],$$

Symmetry property: $\quad f \leftrightarrow g, \quad l \leftrightarrow -l-2$

$$\frac{d\sigma(\phi)}{d\phi} = \frac{2}{\pi k} \left| t_{-1} + 2\sum_{l=0}^{\infty} t_l \cos[(l+1)\phi] \right|^2$$

Bilayer IV

For small wave vectors:

$t_0(k)$ tends to a finite complex number

$$\frac{d\sigma(\phi)}{d\phi} = \frac{8}{\pi k}|t_0(k)|^2 \cos^2 \phi$$

Resistivity estimation like for long-ranged potential in the single-layer graphene:

$(h/4e^2)n_{\mathrm{imp}}/n.$ No logarithmic corrections!

Coulomb potential

$$V_0(\mathbf{r}) = \frac{Ze^2}{\epsilon r}$$

**Scattering phases are energy independent.
Scattering cross section σ is proportional to 1/k
(concentration independent mobility as in experiment)
(Nomura & MacDonald, PRL 2006; Ando, JPSJ 2006 –
linear screening theory)**

**Nonlinear screening (MIK, PRB 2006); exact solution of
Coulomb-Dirac problem (Shytov, MIK & Levitov PRL
2007; Pereira & Castro Neto PRL 2007; Novikov PRB 2007
and others). Relativistic collapse for supercritical
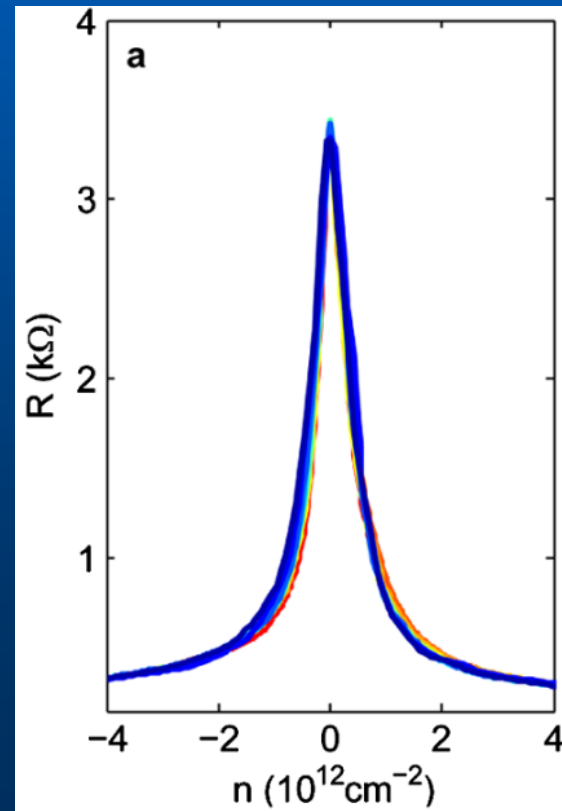charges!!!**

Experimental situation
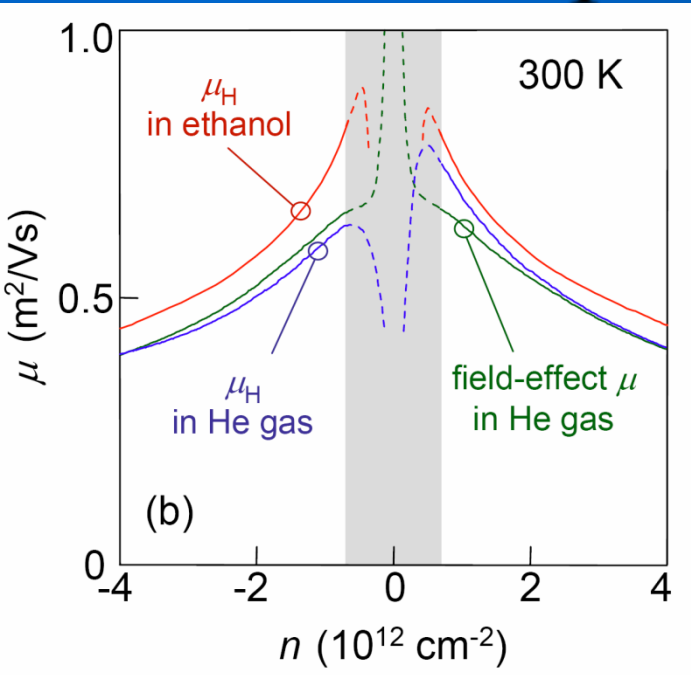
Ponomarenko et al, PRL 102, 206603 (2009)
Almost no sensitivity to screened medium (ethanol, $\kappa = 25$), glycerol, water and to dielectric constant of substrate

Couto et al, PRL 107, 225501 (2011)

Graphene on $SrTiO_3$:
Very large and strongly T-dependent κ (from 200-300 @RT to 5000 at $T = 0$)
Almost no temperature dependence of transport

Clusterization

Explanation: clusterization of charge impurities???
MIK, Guinea and Geim, PR B 79, 195426 (2009)
For some charge impurities (e.g., Na, K…) barriers are low
(< 0.1 eV) and there is tendency to clusterization

Exp. review: Caragiu & Finberg, JPCM 17, R995 (2005)
Calculations: Chan, Neaton & Cohen, PR B 77, 235430 (2008)

Simplest model: just circular cluster, constant
potential (shift of chemical potential)

$$g = \frac{e^2}{h} k_F l \sim \begin{cases} \frac{e^2}{h} \frac{1}{n_C R^2} & k_F R \ll 1 \\ \frac{e^2}{h} \frac{k_F^2}{n_C} & k_F R \gg 1 \end{cases}$$

Correct concentration dependence, weakening of scattering in
two order of magnitude due to clusterization!

Clusterization II

Positions *t* (top of C atom) vs *h* (middle of hexagon):
Covalent (neutral impurities usually have high barriers,
Ionic (charged) impurities have lower barriers
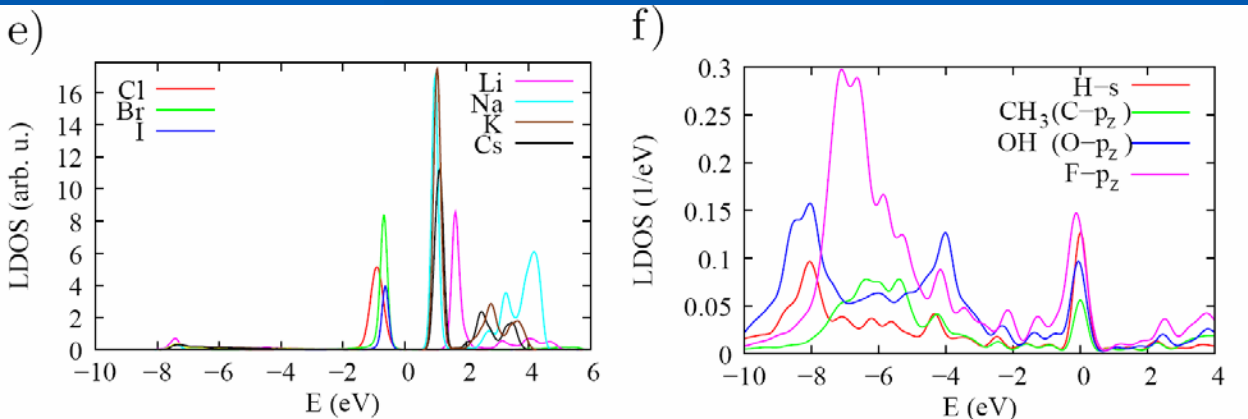
Resonant impurities survive, charged impurities form clusters?

Still under discussions!

Table II: Migration barriers ΔE and minimum energy site for ionically and covalently bond impurities.

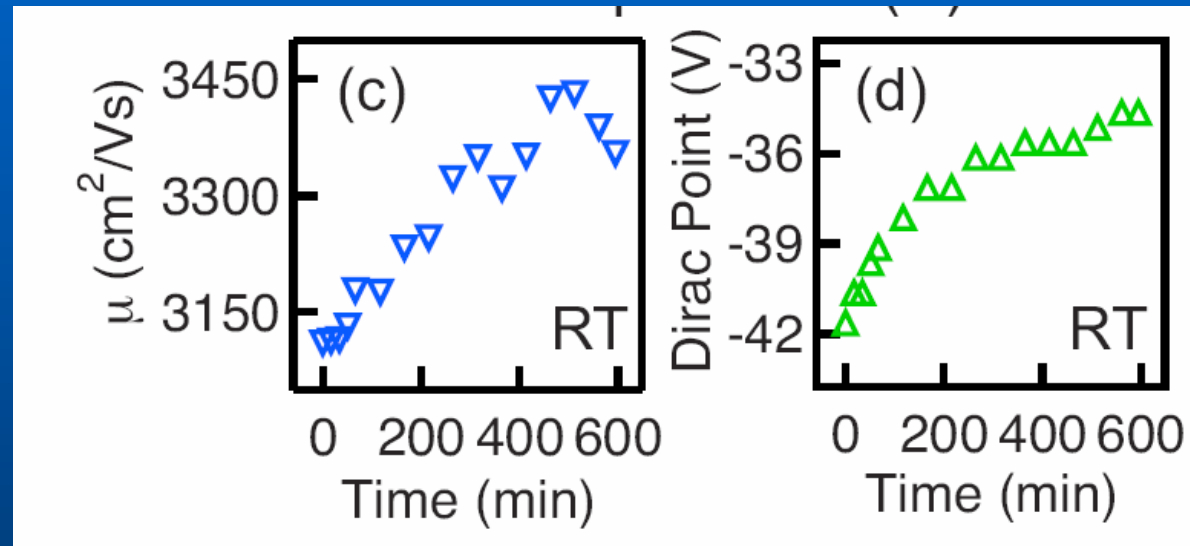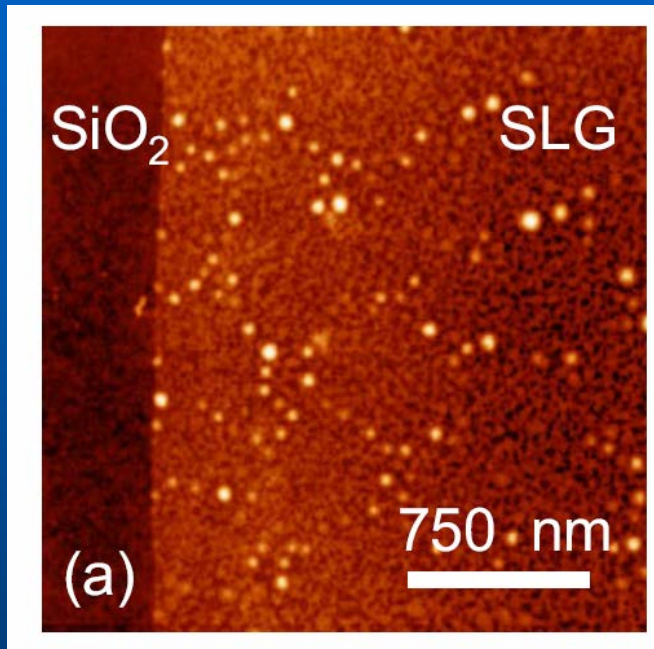|	site	ΔE (eV)		site	ΔE (eV)		site	ΔE (eV)
H	t	1.01	Li	h	0.31	Cl	t,b	0.00
CH$_3$	t	0.63	Na	h	0.09	Br	t,b	0.00
OH	t	0.53	K	h	0.06	I	t,b	0.00
F	t	0.29	Cs	h	0.04			

Clusterization III

Experiment: Au clusterization on graphene
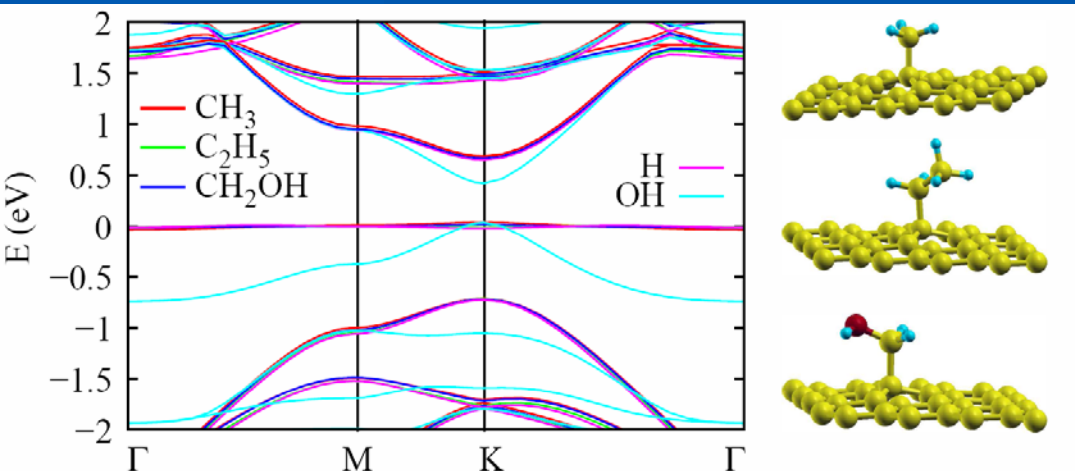McCreary et al, PRB 81, 115453 (2010)

Gold cluster formation
on graphene (AFM)

Mobility increases, Dirac point shifts
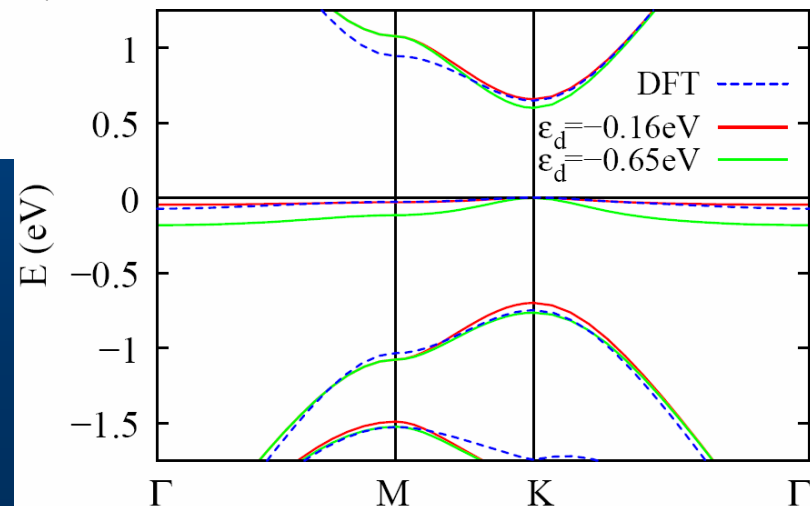
Resonant impurities

Experimentally: exfoliated graphene is polluted by organic stuff; mobility correlates with the forbidden Raman *D* peak (Manchester group 2010)

Wehling, Yuan, Lichtenstein, Geim & MIK, PRL 105, 056802 (2010)

C-C bond or C-H bond: resonant scatterers

Pollution by organics, C-C bridges (one per 1000 to 10000 atoms is enough); hidden from STM!

Resonant impurities II

Effective hybridization model

$$\hat{H} = \sum_{ij} t_{ij}\, \hat{c}_i^+ \hat{c}_j + \sum_{ij} \gamma_{ij}\left(\hat{c}_i^+ \hat{d}_j + \hat{d}_j^+ \hat{c}_i\right) + E_{\mathrm{d}}\sum_i \hat{d}^+_i \hat{d}_i$$

$$\gamma_{ij} = \gamma \delta_{ij}$$ Effective on-site potential $$V(E) = \frac{\gamma^2}{E - E_{\mathrm{d}}}$$

Very strong

Resonant impurities are like vacancies $$\gamma^2 \gg |E_{\mathrm{d}}||t|$$

Parameters from DF calculations

$\gamma = 2t$ for all kind of defects under consideration

$E_d = -t/16$ for hydrogen and organic groups (*C-C* bonds)

$E_d = -t$ for fluorine and *OH* $E_d = 0$ for vacancies

Resonant impurities III
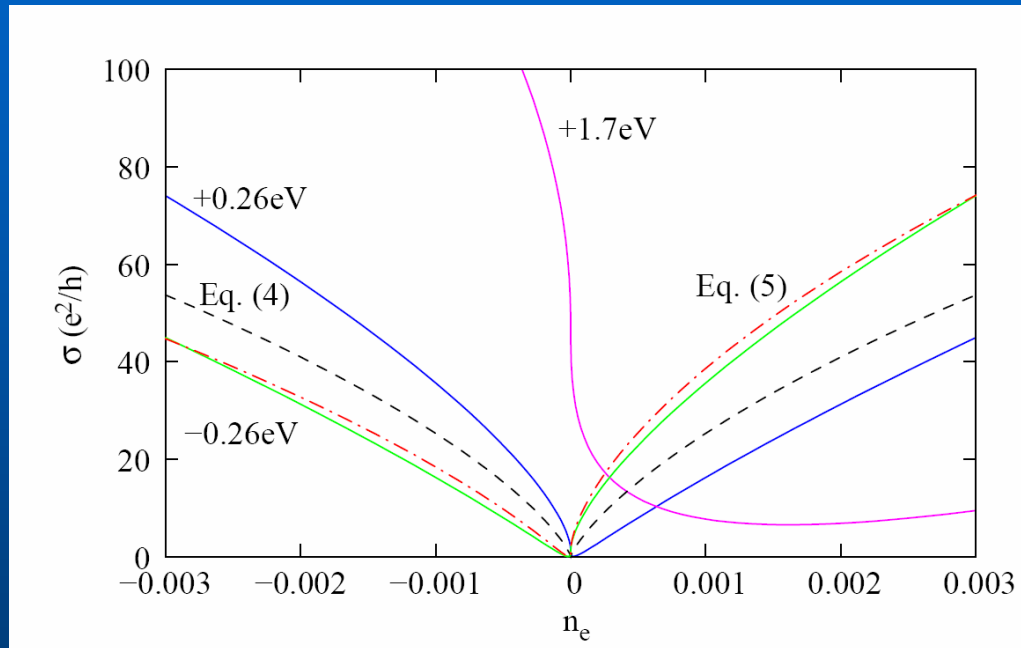
Boltzmann equation

Figure 2: (Color online) Conductivity σ in the Boltzmann approach as function of charge carrier concentration n_e (in units of electrons per atom) for different impurities: Impurities with hybridization $V = 2t = 5.2\,\text{eV}$ and on-site energies $\epsilon_d = -0.26$, 0.26, and $1.7\,\text{eV}$ in concentration $n_i = 0.1\%$.

For symmetric resonances

$$\sigma \;\approx\; (2e^2/h)\frac{2}{\pi}\frac{n_e}{n_i}\ln^2\left|\frac{E_F}{D}\right|$$

Confirmed by many experiments (e.g., for graphene on SrTiO$_3$)

Asymmetry

$$\sigma \propto \left(q_0 \pm k_F \ln k_F R\right)^2$$

Numerical simulations

The method: Yuan, De Raedt & MIK, PR B 82, 115448 (2010)
Applications: Yuan, De Raedt & MIK, PR B 82, 235409 (2010) bi- and trilayer
Yuan, Roldan & MIK, PR B 84, 035439 (2010) plasmons and EELS
Yuan, Roldan & MIK, PR B 84, 125435 (2010) bi- and trilayer, Landau spectrum
Yuan, Roldan, De Raedt & MIK, PR B 84, 195418 (2011) optics
Yuan, Roldan & MIK, Sol. St. Comm. (2012) plasmons in magnetic field
Yuan, Wehling, Lichtenstein & MIK (2012) static screening and localization

Basic idea: calculation of evolution operator via Chebyshev
polynom expansion plus average over some random initial state

$$\left|\varphi(t)\right\rangle = \tilde{U}\left|\varphi(0)\right\rangle = e^{-itH}\left|\varphi(0)\right\rangle$$

$$e^{-izx} = J_0(z) + 2\sum_{m=1}^{\infty}(-i)^m J_m(z)T_m(x)$$

$$T_m(x) = \cos[m\arccos(x)], x \in [-1,1]$$
$$T_{m+1}(x) + T_{m-1}(x) = 2xT_m(x)$$

$$\hat{T}_m(\hat{H}) = (-i)^m T_m(\hat{H}) = (-i)^m \sum_{n=1}^{N} T_m(\hat{E}_n)\left|E_n\right\rangle\left\langle E_n\right|$$

$$\hat{T}_0(\hat{H})\left|\phi\right\rangle = \left|\phi\right\rangle$$
$$\hat{T}_1(\hat{H})\left|\phi\right\rangle = -i\hat{H}\left|\phi\right\rangle$$
$$\hat{T}_{m+1}(\hat{H})\left|\phi\right\rangle = -2i\hat{H}\hat{T}_m(\hat{H})\left|\phi\right\rangle + \hat{T}_{m-1}(\hat{H})\left|\phi\right\rangle$$

Density of states
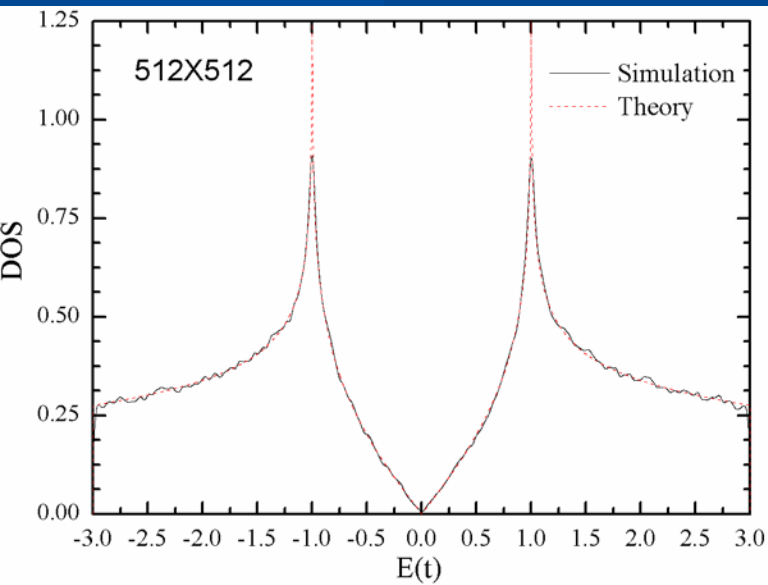
A. Hams and H. De Raedt, PR E 62, 4365 (2000)
S. Yuan, H. De Raedt & MIK Phys. Rev. B 82, 115448 (2010)

$$\rho(E) = \frac{1}{N} \sum_{n=1}^{N} \delta(E - E_n)$$

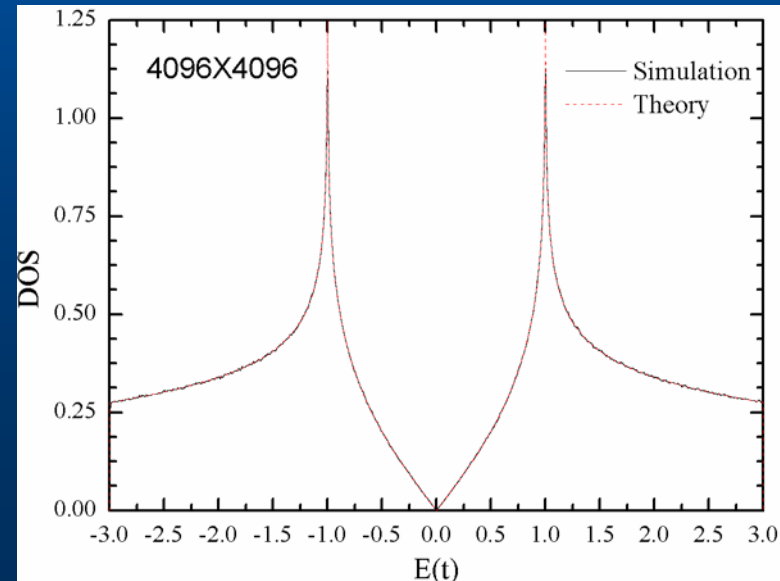$$\left|\varphi(0)\right\rangle = \sum_n a_n \left|E_n\right\rangle = \sum_i b_i c_i^+ \left|0\right\rangle_i$$

Normalized Random Complex Numbers

$$\frac{1}{2\pi} \int_{-\infty}^{\infty} e^{iEt} \left\langle\varphi(0)\big|\varphi(t)\right\rangle = \sum_n \left|a_n\right|^2 \delta(E - E_n) \approx \rho(E)$$

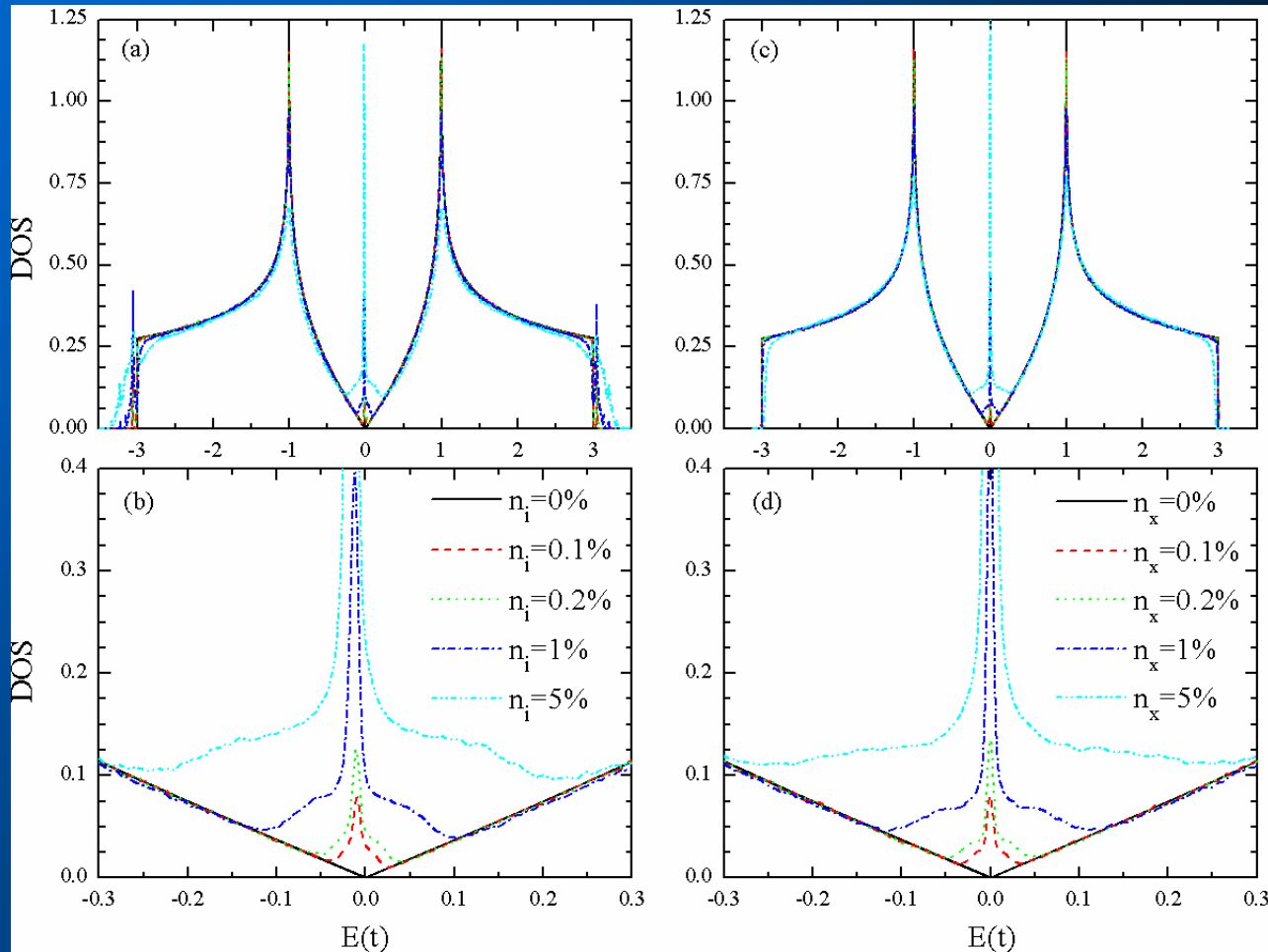10^7 sites!!!

Test: ideal SLG, nearest-neighbour approx. (analytic DOS Is known)

DOS with resonant impurities

Midgap states and impurity band for hydrogen impurities (left) and vacancies (right)

Optics

Kubo Formula :

$$\sigma_{\alpha\beta}(\omega) = \lim_{\varepsilon \to 0^+} \frac{1}{(\omega + i\varepsilon)\Omega} \left\{ -i\left\langle [P_\alpha, J_\beta] \right\rangle + g_{\alpha\beta}(\omega) \right\}$$

$$g_{\alpha\beta}(\omega) = \int_0^\infty dt e^{i(\omega + i\varepsilon)t} \left\langle [J_\alpha(t), J_\beta] \right\rangle$$
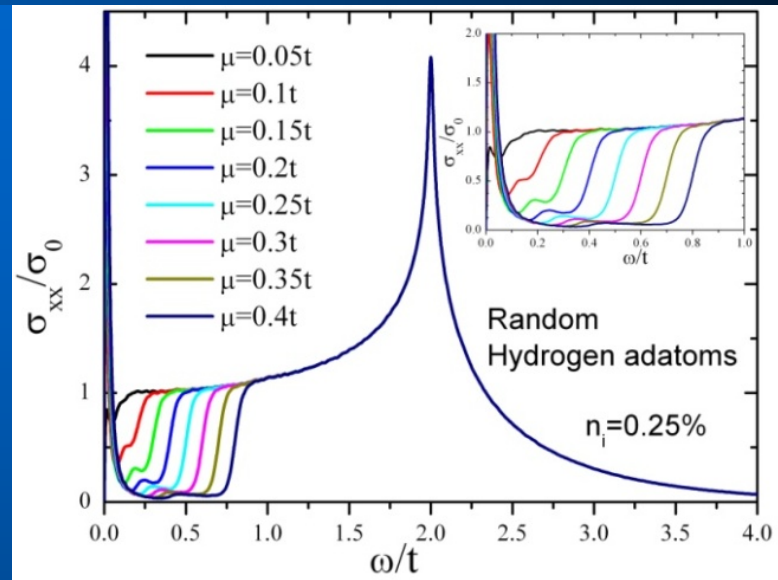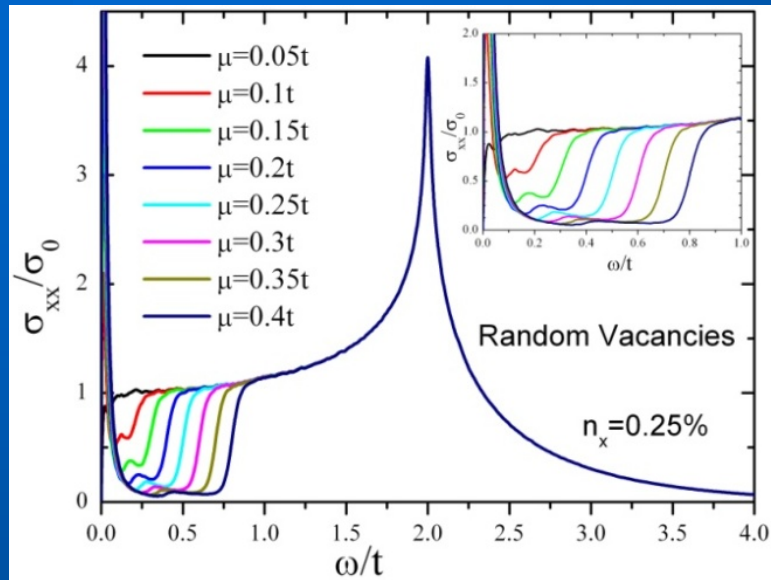
$$\boldsymbol{P} = e\sum_i \boldsymbol{r}_i c_i^+ c_i, \; \boldsymbol{J} = i[\boldsymbol{P}, H] = -ie\sum_i t_{i,j}(\boldsymbol{r}_j - \boldsymbol{r}_i)c_i^+ c_i, \; n_F = \frac{1}{1 + e^{\beta(H-\mu)}}$$

$$\mathrm{Re}\,\sigma_{\alpha\beta}(\omega) = \lim_{\varepsilon \to 0^+} \frac{e^{-\beta\omega} - 1}{\omega\Omega} \int_0^\infty dt e^{-\varepsilon t} \sin \omega t$$

$$\times 2\,\mathrm{Im}\left\langle \varphi \middle| n_F(T, \mu) e^{iHt} J_\alpha e^{-iHt} [1 - n_F(T, \mu)] J_\beta \middle| \varphi \right\rangle$$

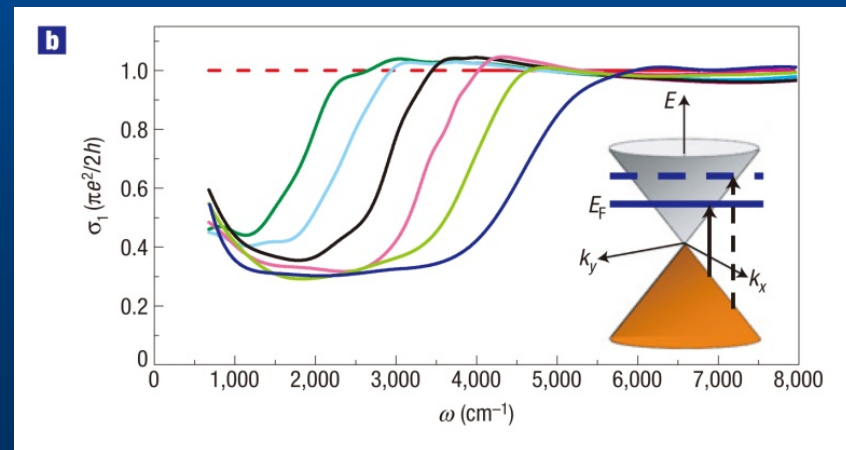φ is a random function as at calculations of DOS

Optics II

Background in IR optics (states in the gap)

Z. Q. Li, *et al.,* Nature Physics **4,** 532(2008)
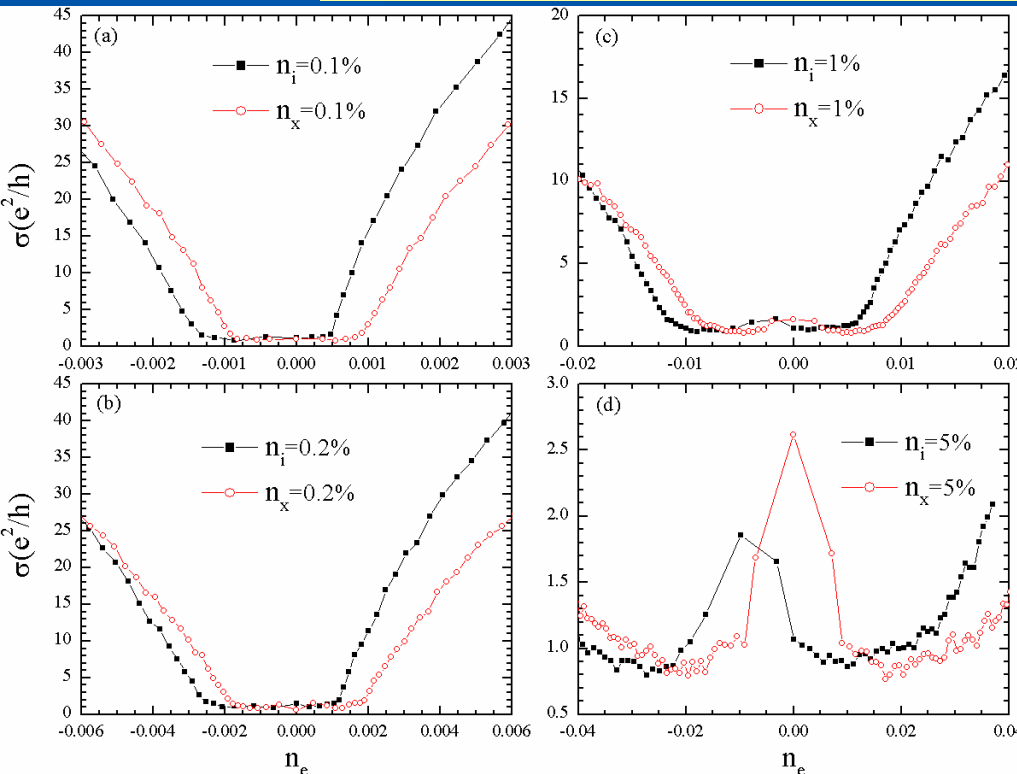
Experiment: defects or many-body?

dc Conductivity

Kubo Formula with $\omega = 0$

$$\sigma(\omega = 0) = -\frac{1}{\Omega} Tr\left\{\frac{\partial f}{\partial H}\int_0^\infty dt \frac{1}{2}\left[\boldsymbol{JJ}(t) + \boldsymbol{J}(t)\boldsymbol{J}\right]\right\}$$

$$\overset{T=0}{\approx} -\frac{1}{\Omega}\frac{\rho(E)}{\langle\varphi|\varepsilon\rangle}\int_0^\infty dt\, \mathrm{Re}\left[e^{-iEt}\langle\varphi|\boldsymbol{J}e^{iHt}\boldsymbol{J}|\varepsilon\rangle\right]$$

Agrees with Boltzmann equation far enough from neutrality point and for small enough defect concentration

Sensitivity to the nearest-neighbor hopping

Quantum capacitance measurements of electron-hole asymmetry and next-nearest-neighbor hopping in graphene

A. Kretinin,[1] G. L. Yu,[2] R. Jalil,[1] Y. Cao,[1] F. Withers,[2] A. Mishchenko,[2] M. I. Katsnelson,[3] K. S. Novoselov,[2] A. K. Geim,[1,2] and F. Guinea[4,5]
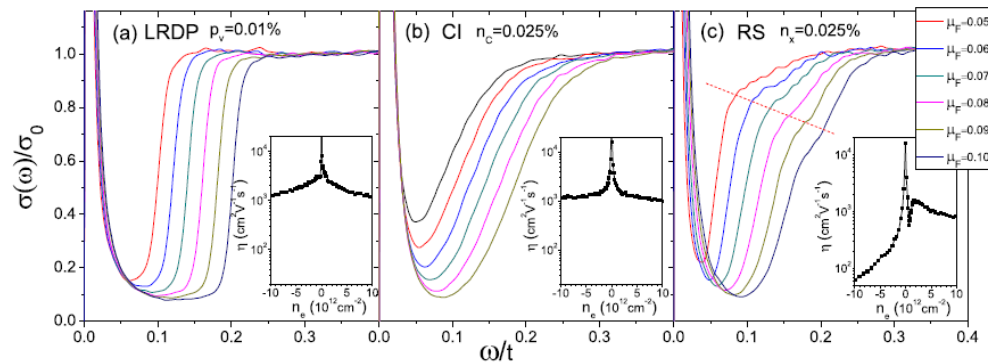
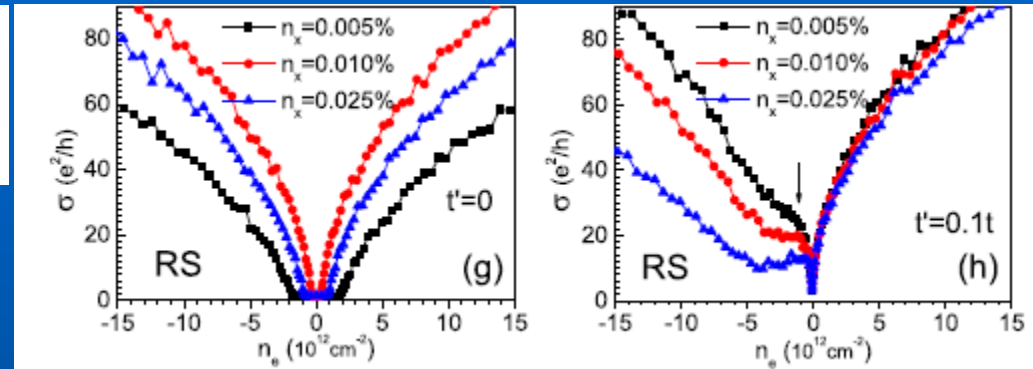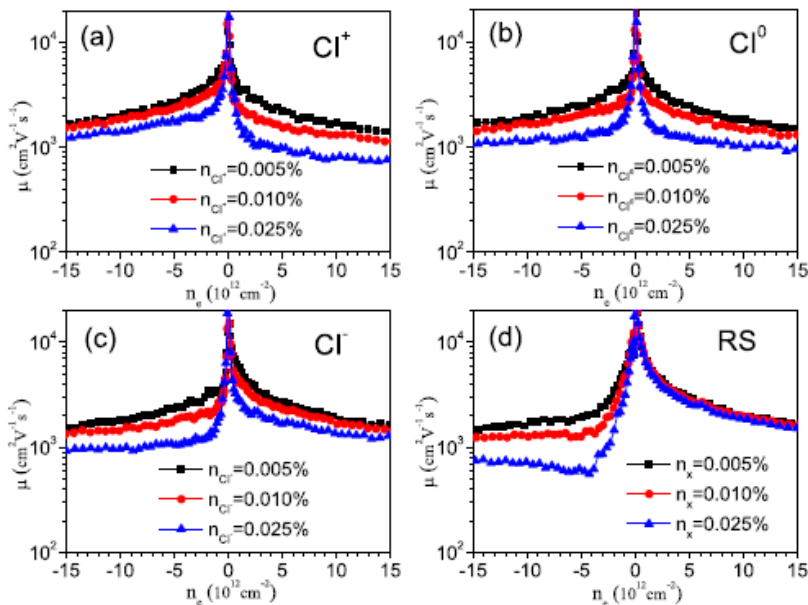$$t' \approx -0.3 \text{ eV} \pm 15\%$$
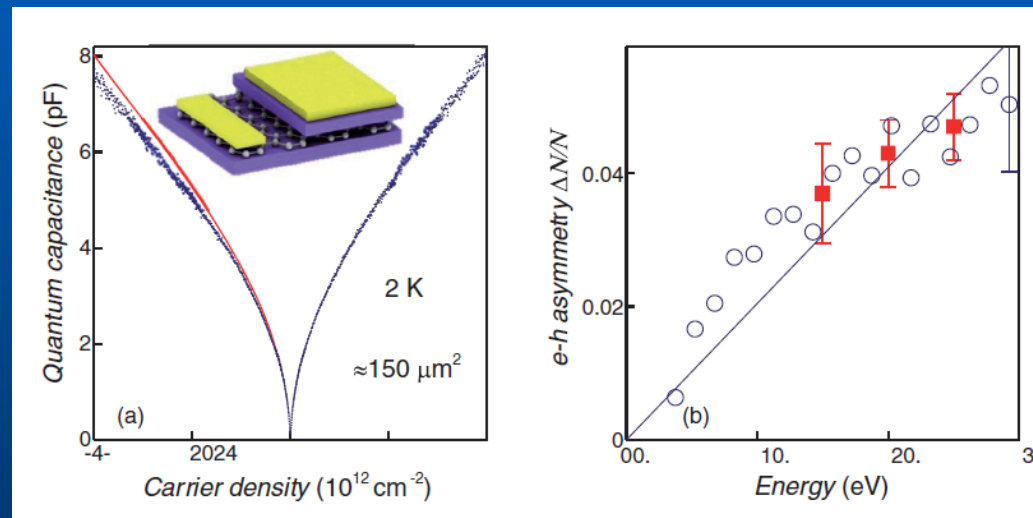
Sensitivity to the nearest-neighbor hopping II

Fingerprints of disorder source in graphene

Pei-Liang Zhao,[1] Shengjun Yuan,[2,*] Mikhail I. Katsnelson,[2] and Hans De Raedt[1]

Strong e-h asymmetry!

IR optics, Landay levels...
RI scattering is quite different
from all other sources

Ripples and puddles I

Gibertini, Tomadin, Polini, Fasolino & MIK, PR B 81, 125437 (2010)

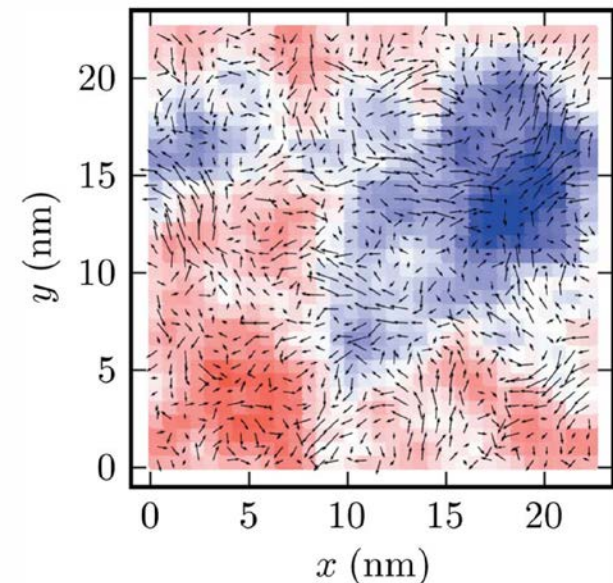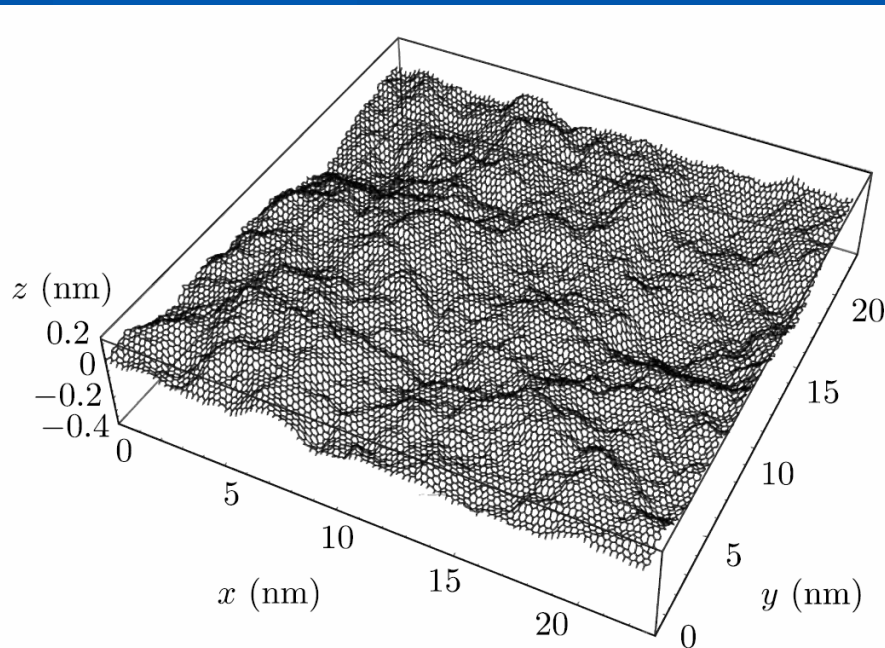Atomic coordinates from atomistic MC simulations for thermal ripples

FIG. 2. (Color online) Average displacements $\overline{\boldsymbol{u}}(\boldsymbol{r})$ calculated as discussed in Sec. II A. The color scale represents the $\hat{z}$ component of the average displacements, varying from -3.0 Å (blue) to $+3.0$ Å (red). The arrows, whose length has been multiplied by a factor ten for better visibility, represent the in-plane components of the average displacements.

Ripples and puddles II

Scalar potential

$$V_1 = g_1(u_{xx} + u_{yy})$$

Vector potential

$$V_2 = g_2(u_{xx} - u_{yy} + 2iu_{xy})$$

Distribution of potentials
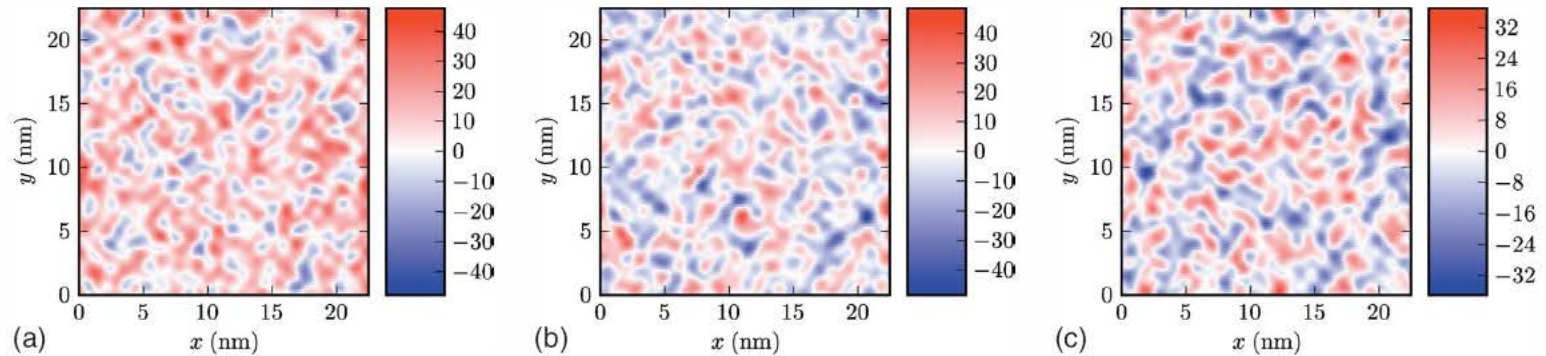

FIG. 3. (Color online) Left panel: color plot of the scalar potential $V_1(r)$ (in units of meV) calculated using Eq. (2) with $g_1=3$ eV. Central panel: the real part of the potential $V_2(r)$ (in units of meV) calculated using Eq. (3). Right panel: the imaginary part of the potential $V_2(r)$ (in units of meV).
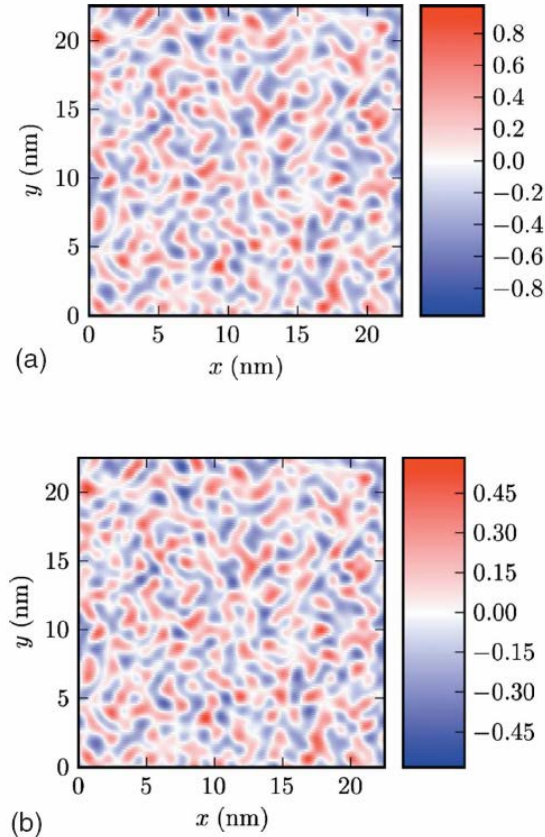
Ripples and puddles III

(a)

(b)

FIG. 4. (Color online) Top panel: fully self-consistent electronic density profile $\delta n(r)$ (in units of 10^{12} cm^{-2}) in a corrugated graphene sheet. The data reported in this figure have been obtained by setting $g_1 = 3$ eV, $\alpha_{ee} = 0.9$ (this value of α_{ee} is the commonly used value for a graphene sheet on a SiO$_2$ substrate), and an average carrier density $\bar{n}_c \simeq 0.8 \times 10^{12}$ cm^{-2}. Bottom panel: same as in the top panel but for $\alpha_{ee} = 2.2$ (this value of α_{ee} corresponds to suspended graphene).

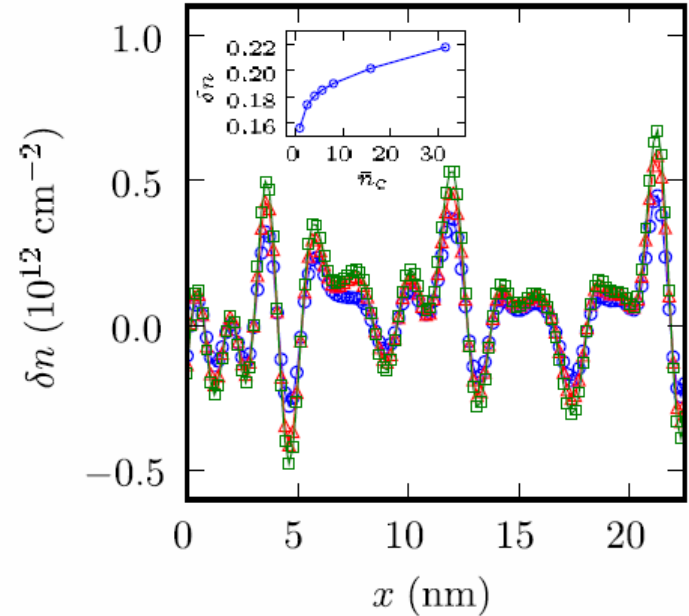FIG. 9. (Color online) One-dimensional plots of the self-consistent density profiles (as functions of x in nm for $y = 21.1$ nm) for different values of doping: $\bar{n}_c \simeq 0.8 \times 10^{12}$ cm^{-2} (circles), $\bar{n}_c \simeq 3.96 \times 10^{12}$ cm^{-2} (triangles), and $\bar{n}_c \simeq 3.17 \times 10^{13}$ cm^{-2} (squares). The data reported in this figure have been obtained by setting $g_1 = 3$ eV and $\alpha_{ee} = 2.2$. The inset shows $\delta n(r)$ (in units of 10^{12} cm^{-2}) at a given point r in space as a function of the average carrier density $\bar{n}_c$ (in units of 10^{12} cm^{-2}).

Ripples and puddles IV

Graphene on SiO$_2$

Gibertini, Tomadin, Guinea, MIK & Polini PR B 85, 201405 (2012)
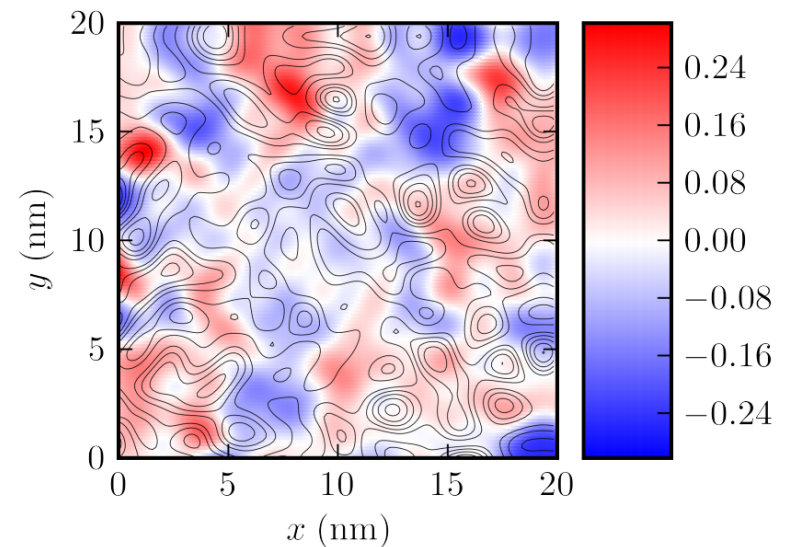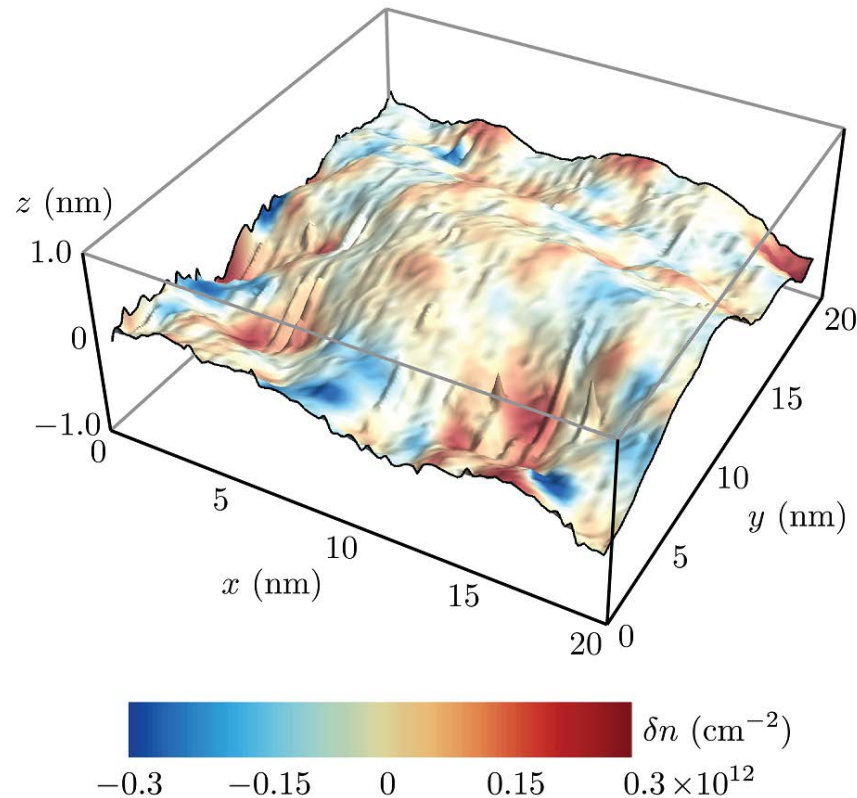Experimental STM data: V.Geringer et al (M.Morgenstern group)

FIG. 3: (Color online) Fully self-consistent induced carrier-density profile $\delta n(\boldsymbol{r})$ (in units of 10^{12} cm^{-2}) in the corrugated graphene sheet shown in Fig. 1. The data reported in this figure have been obtained by setting $g_1 = 3$ eV, $\alpha_{\rm ee} = 0.9$, and an average carrier density $\bar{n}_{\rm c} \approx 2.5 \times 10^{11}$ cm^{-2}. The thin solid lines are contour plots of the curvature $\nabla_{\boldsymbol{r}}^2 h(\boldsymbol{r})$. Note that there is no simple correspondence between topographic out-of-plane corrugations and carrier-density inhomogeneity.

Scattering by ripples

Scattering by random vector and scalar potential:

$$H' = \sum_{\mathbf{pp}'} \Psi_{\mathbf{p}}^{\dagger} V_{\mathbf{pp}'} \Psi_{\mathbf{p}'}$$

$$V_{\mathbf{pp}'} = V_{\mathbf{pp}'}^{(0)} + A_{\mathbf{pp}'}^{(x)} \sigma_x + A_{\mathbf{pp}'}^{(y)} \sigma_y$$

$$\frac{1}{\tau} = \frac{4\pi}{\hbar N(\varepsilon_F)} \sum_{\mathbf{pp}'} \delta\left(\varepsilon_{\mathbf{p}} - \varepsilon_F\right) \delta\left(\varepsilon_{\mathbf{p}'} - \varepsilon_F\right) \left(\cos\theta_{\mathbf{p}} - \cos\theta_{\mathbf{p}'}\right)^2 \left|W_{\mathbf{pp}'}\right|^2$$

$$W_{\mathbf{pp}'} = V_{\mathbf{pp}'}{}^{(0)} \frac{1 + \exp\left[-i\left(\theta_{\mathbf{p}} - \theta_{\mathbf{p}'}\right)\right]}{2} + $$
$$+ \frac{1}{2}\left[\left(A_{\mathbf{pp}'}^{(x)} + iA_{\mathbf{pp}'}^{(y)}\right)\exp\left(-i\theta_{\mathbf{p}}\right) + \left(A_{\mathbf{pp}'}^{(x)} - iA_{\mathbf{pp}'}^{(y)}\right)\exp\left(i\theta_{\mathbf{p}'}\right)\right]$$
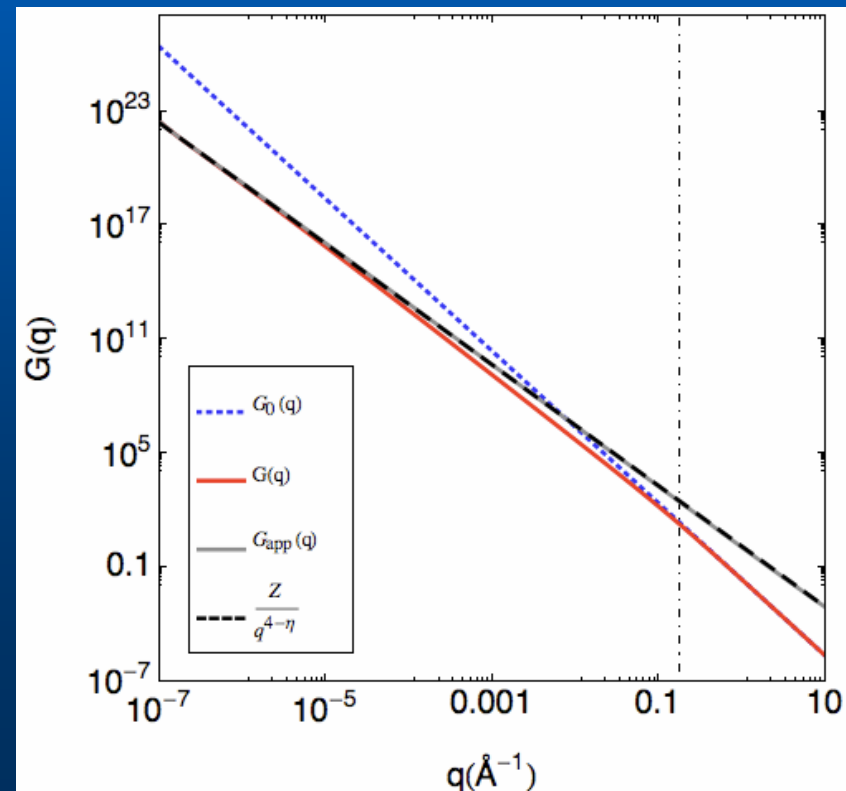
Scattering by ripples II

Estimations:

$$\frac{1}{\tau} \simeq \frac{2\pi N\left(\varepsilon_F\right)}{\hbar} \left(\left\langle V_{\mathbf{q}}^{(0)} V_{-\mathbf{q}}^{(0)} \right\rangle + \left\langle \mathbf{A}_{\mathbf{q}} \mathbf{A}_{-\mathbf{q}} \right\rangle \right)_{q \approx k_F}$$

$$\langle \mathbf{V}_q \mathbf{V}_{-q} \rangle \approx \left(\frac{\hbar v_{\mathrm{F}}}{a}\right)^2 \sum_{\mathbf{q}_1 \mathbf{q}_2} \langle h_{\mathbf{q}-\mathbf{q}_1} h_{\mathbf{q}_1} h_{-\mathbf{q}+\mathbf{q}_2} h_{-\mathbf{q}_2} \rangle [(\mathbf{q}-\mathbf{q}_1)\cdot\mathbf{q}_1][(\mathbf{q}-\mathbf{q}_2)\cdot\mathbf{q}_2]$$

Self-consistent screening approximation (Zakharchenko, Roldan, Fasolino & MIK)

"Harmonic" ripples @ RT

$$k_F \geq q^*$$

Scattering by ripples III

$$\rho_r \approx \frac{h}{4e^2} \frac{(k_\mathrm{B} T/\kappa a)^2}{n} \Lambda$$

Λ depends logarithically on k_F and q^*
(Geim & MIK, 2008)

Quantum theory: two-phonon processes
At high T roughly the same result
Strong sensitivity to the strains
via frequency of flexural phonons:

$$\omega_{\vec{\mathbf{q}}}^F(\vec{\mathbf{r}}) = |\vec{\mathbf{q}}| \sqrt{\frac{\kappa}{\rho}|\vec{\mathbf{q}}|^2 + \frac{\lambda}{\rho} u_{ii}(\vec{\mathbf{r}}) + \frac{2\mu}{\rho} u_{ij}(\vec{\mathbf{r}}) \frac{q_i q_j}{|\vec{\mathbf{q}}|^2}}$$

Quantitative results and comparison with experiment on freely suspended samples:
Castro, Ochoa, MIK, Gorbachev, Elias, Novoselov, Geim & Guinea, PRL 105, 266601 (2010)

Flexural phonons
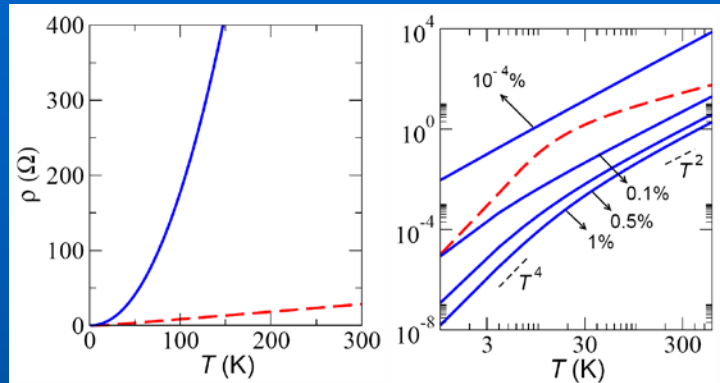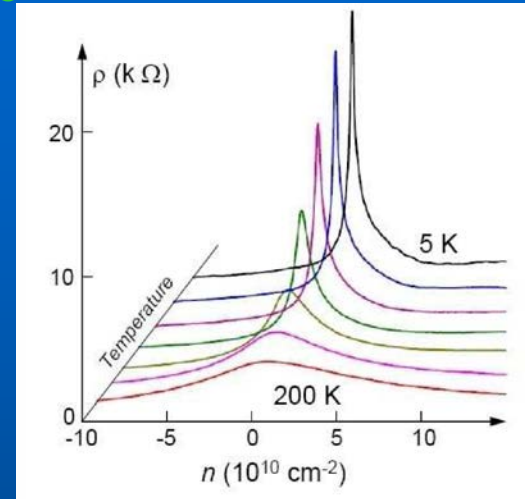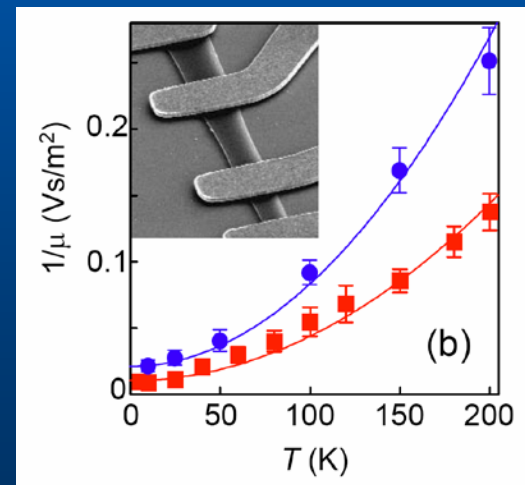
H.Ochoa, E.Castro, MIK, F.Guinea 2010

FIG. 2: (Color online). Left: Contribution to the resistivity from flexural phonons (blue full line) and from in plane phonons (red dashed line). Right: Resistivity for different amounts of strain. Note that the in plane contribution (broken red line) shows a crossover from a low to a high temperature regime. In both cases, the electronic concentration is $n = 10^{12} cm^{-2}$.

1. Mobility at RT cannot be higher than on substrate for the flexural phonons only
2. It can be essentially increased by applying a strain

Exper. data

T-dependence of mobility for two samples

Qualitative agreement between classical and quantum theory @ RT

Take-away message from the talk

Three candidates to the main scattering mechanism (long range is necessary!!!)

Coulomb centers? (I personally doubt: no effect of high-kappa environment, tendencies to clusterize for ionic impurities)

Ripples? (aka flexural phonons, probably the main mechanism for suspended graphene). For graphene on substrate: need quenching mechanism

Resonant impurities? Carbon-carbon bonds between garbage and graphene (Strong electron-hole symmtery is a fingerprint)

Main collaborators

Andre Geim, Kostya Novoselov (Manchester)

Shengjun Yuan, Annalisa Fasolino, Kostya
    Zakharchenko, Jan Los (Nijmegen)

Sasha Lichtenstein, Tim Wehling (Hamburg)

Paco Guinea, Rafael Roldan, Eduardo Castro, Hector
    Ochoa (Madrid)

Marco Polini (Pisa)